Structural Changes Associated with Electron-Transfer Reactions. One- *vs* Two-Step Reactions in the Oxidation of $W(\eta^5\text{-}C_5(CH_3)_5)(CH_3)_4$

Susan A. Lerke[1] and Dennis H. Evans*

Contribution from the Department of Chemistry and Biochemistry, University of Delaware, Newark, Delaware 19716

Received August 21, 1995[⊗]

Abstract: In accord with the original interpretation of Liu *et al.* (*J. Am. Chem. Soc.* **1987**, *109*, 4282−4291), it has been demonstrated that electrochemical oxidation of the title compound in methylene chloride proceeds by a two-step process by which the square-pyramidal neutral reactant (SP) is oxidized to a cation of similar structure (SP^+) followed by isomerization to the preferred trigonal-bipyramidal cation (TBP^+). A combination of slow cyclic voltammetry near room temperature and fast scan experiments at low temperature has allowed determination of the thermodynamic and kinetic parameters for the conversion of SP^+ to TBP^+ ($\Delta H° = -6.05$ kcal/mol; $\Delta S° = -3.97$ cal mol^{-1} K^{-1}; $\Delta G°*_{298} = 9.5$ kcal/mol). The reversible formal potential for the SP/SP^+ couple is +1.20 V *vs* cobaltocenium/cobaltocene in the same solvent and the reversible formal potential for the direct one-step oxidation of SP to TBP^+ is 0.99 V, *i.e.*, the direct oxidation requires 5 kcal/mol less energy than the two-step reaction. The fact that the reaction actually proceeds *via* the two-step pathway is explained by a large barrier to the direct oxidation, calculated to be greater than about 12 kcal/mol. It is argued that this large barrier is reasonable in view of the expected contribution from the outer and inner reorganization energies.

Introduction

There are many instances in which a significant structural change is associated with an electron-transfer reaction. Such structural changes include isomerizations and changes in conformation. If the structural modification is a discrete chemical reaction that follows the electron-transfer step, the overall reaction can be called a two-step electron-transfer reaction. However, there are a number of cases in which quite substantial structural changes apparently occur in concert with the electron trnasfer, *i.e.*, electron transfer and structural change are concomitant and the reaction can be termed a one-step or direct electron transfer. Examples of such cases include flattening of the cyclooctatetraene ring upon introduction of an electron,[2] change in the intercarbonyl dihedral angle accompanying reduction of cyclic 1,2-diketones,[3] changes in various bond lengths and the geometry at the nitrogen atoms seen on oxidation of tetraalkylhydrazines,[4] and a *potpourri* of structural adjustments associated with the two-electron oxidation of some bis-enamines.

In order to demonstrate that a two-step electron-transfer reaction is occurring, it is necessary that an intermediate be present that is not too high in energy compared with the ultimate product and which is separated from that product by a sufficient barrier to give the intermediate a sufficient lifetime to allow detection. The structural change is usually a type of isomerization and there are many examples of the reactions of organic and organometallic species that fall in this class.[6]

Scheme 1

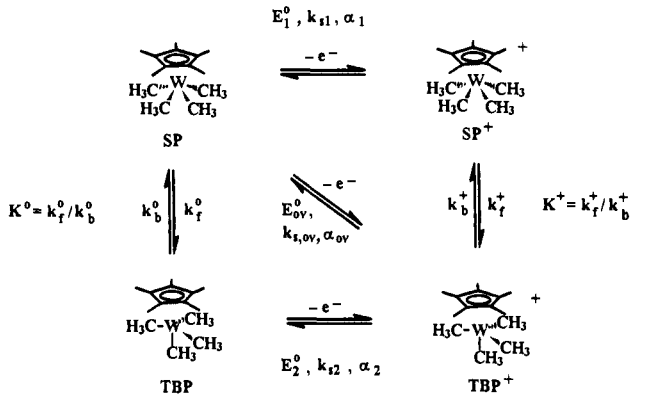

It is of interest to explore the boundary territory separating one- and two-step reactions, *i.e.*, one-step reactions with very large structural change that might be expected to occur in two sequential steps or two-step reactions where the structural modification appears to be modest and which might be a candidate for concomitant electron transfer and structural change.

In this regard, we were drawn to the report[7] that $W(\eta^5\text{-}C_5(CH_3)_5)(CH_3)_4$ and its cation constitute a half reaction in which a relatively modest change occurs in a two-step reaction. The neutral compound adopts a square-pyramidal structure (Scheme 1) while the cation exists as a pseudo trigonal bipyramid formed by moving one methyl group to an axial position and raising the other three to equivalent equatorial positions. Preliminary

[⊗] Abstract published in *Advance ACS Abstracts*, November 1, 1995.

(1) Present address: Sanofi Winthrop, Inc., 1250 South Collegeville Road, P.O. Box 5000, Collegeville, PA 19426−0900.

(2) Allendoerfer, R. D.; Rieger, P. H. *J. Am. Chem. Soc.* **1965**, *87*, 2336−2344.

(3) Brielbeck, B.; Rühl, J. C.; Evans, D. H. *J. Am. Chem. Soc.* **1993**, *115*, 11898−11905.

(4) (a) Nelsen, S. F. *Acc. Chem. Res.* **1981**, *14*, 131−138. (b) Nelsen, S. F. In *Molecular Structures and Energetics*; Liebman, J. F., Greenberg, A., Eds.; VCH Publishers, Inc.: Deerfield Beach, FL, 1986; Vol. 3, Chapter 1, pp 1−86. (c) Nelsen, S. F.; Blackstock, S. C.; Kim, Y. *J. Am. Chem. Soc.* **1987**, *109*, 677−682.

(5) Hu, K.; Evans, D. H. *J. Phys. Chem.* submitted for publication.

(6) (a) Geiger, W. E. In *Progress in Inorganic Chemistry*; Lippard, S. J., Ed.; John Wiley and Sons: New York, 1985; Vol. 33, pp 275−352. (b) Evans, D. H.; O'Connell, K. M. In *Electroanalytical Chemistry*; Bard, A. J., Ed.; Marcel Dekker: New York, 1986; Vol. 14, pp 113−207.

(7) Liu, A. H.; Murray, R. C.; Dewan, J. C.; Santarsiero, B. D.; Schrock, R. R. *J. Am. Chem. Soc.* **1987**, *109*, 4282−4291.

0002-7863/95/1517-11768$09.00/0

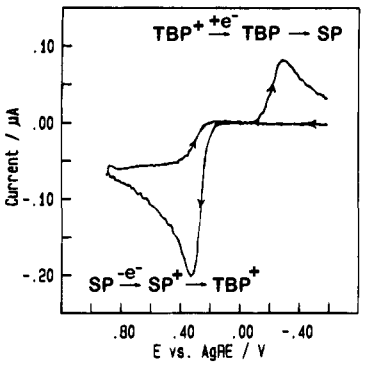

Figure 1. Background-corrected cyclic voltammogram of *ca.* 10 mM $W(\eta^5\text{-}C_5(CH_3)_5)(CH_3)_4$ in methylene chloride containing 0.40 M Bu_4NPF_6. Conditions: 10-μm-diameter platinum-disk electrode, 500 V/s, 25 °C.

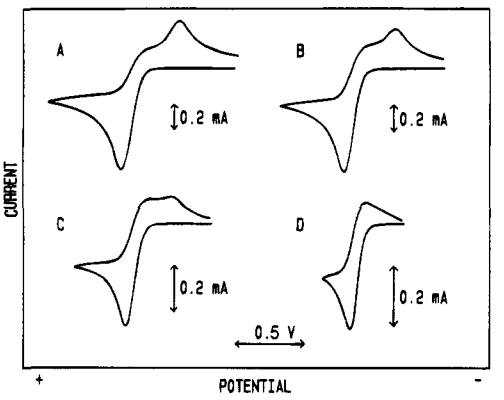

Figure 2. Effect of scan rate on voltammetry of *ca.* 5 mM $W(\eta^5\text{-}C_5(CH_3)_5)(CH_3)_4$ in methylene chloride containing 0.40 M Bu_4NPF_6. Conditions: (A–D) 0.70-cm-diameter platinum-disk electrode, 308 K; (A) 0.20 V/s, E_i (initial potential) = +0.23 V *vs* cobaltocenium/cobaltocene; (B) 0.10 V/s, E_i = +0.33 V; (C) 0.05 V/s, E_i = +0.44 V; (D) 0.02 V/s, E_i = +0.63 V.

electrochemical data were presented which were interpreted in terms of a two-step mechanism, oxidation of the square-pyramidal neutral (SP) to a cation of similar geometry (SP^+) followed by isomerization to the more stable form of the cation, TBP^+ (Scheme 1). No direct evidence for the intermediacy of SP^+ was presented in the original paper.[7] Reports of the properties and uses of these compounds continue[8] though no other studies of the electron-transfer reactions have been reported.

In this paper we present a more complete quantitative characterization of the thermodynamics and kinetics of this interesting reaction and discuss the ramifications of this system in terms of defining the boundary region separating one- and two-step electron-transfer reactions.

Results

A cyclic voltammogram for $W(\eta^5\text{-}C_5(CH_3)_5)(CH_3)_4$ is shown in Figure 1. This response is typical for room temperature experiments conducted at scan rates exceeding about 10 V/s. A single oxidation peak is seen at +0.3 V *vs* AgRE and a reduction peak appears at −0.3 V on the negative-going scan. This result is in agreement with that reported by Liu *et al.*[7] and their assignments of the reactions occurring at each peak are indicated in Figure 1. The oxidation is thought to proceed from SP to SP^+ followed by rapid isomerization giving TBP^+. Likewise, the reduction of TBP^+ gives TBP which also rapidly converts to the stable form of the neutral compound, SP. It should be noted that a qualitatively identical response would be seen for the direct one-step electron-transfer reaction (diagonal in Scheme 1) if that reaction showed sluggish electron-transfer kinetics.

Double cycles of the SP voltammogram (not shown) feature sequential peaks whose heights are well accounted for by simulation (see below) assuming no loss of TBP^+ or other competing reactions.

Rejection of the one-step electron-transfer mechanism was clearly indicated by results obtained at slower scan rates. The qualitative effect is illustrated in Figure 2, where at 0.2 V/s (curve A) a new cathodic process is observed as a shoulder on the main reduction peak and this shoulder is situated at potentials close to the oxidation peak. At smaller scan rates and/or higher temperatures, the shoulder grows at the expense of the main reduction peak (curves B and C; 0.10 and 0.05 V/s, respectively) until it becomes the only cathodic feature (curve D, 0.02 V/s). At this point, the voltammogram is identical in shape to a reversible one-electron oxidation of SP to SP^+. (It should be noted that the voltammogram at 0.02 V/s is affected by convection so the data are unsuitable for analysis by digital simulation.)

The explanation for this behavior is to be found in the reversibility of the isomerization reaction of the cations. As will become clear in the subsequent results, the equilibrium constant for isomerization strongly favors TBP^+ (*i.e.* $K^+ \gg 1$, Scheme 1) and the rate constant, k_f^+, is large. Therefore, the oxidation process is described by the sequence SP → SP^+ → TBP^+ and the species with the favored cationic structure, TBP^+, is rapidly produced at the electrode. How then can current be seen on the negative-going sweep at potentials where the unfavored cation, SP^+, is reduced? As K^+ is finite, a small concentration of SP^+ exists near the electrode and it will be reduced on the return sweep of the voltammogram. Furthermore, the rate constant for the reverse isomerization reaction, k_b^+, is large enough to form SP^+ from TBP^+ at a significant rate thus supplying more SP^+ to be reduced at the electrode. Given a slow enough scan rate (or a higher temperature which increases the rate constants), the TBP^+ formed on the first half-cycle can be rapidly reduced on the return sweep giving a diffusion-controlled cathodic peak by the reaction pathway $TBP^+ \rightarrow SP^+ \rightarrow SP$.

In cases where K^+ is large, it is only possible to extract a grouped parameter, $K^+/(k_f^+)^{1/2}$, from analysis of the voltammetric data.[9] Fitting the voltammograms by digital simulation[9] was carried out for a series of scan rates from 50 to 500 mV/s at each of four temperatures. The values of $K^+/(k_f^+)^{1/2}$ so obtained are listed in Table 1. An example of the quality of the fit is shown in Figure 3, where the dashed curve is the simulation. Values of the other simulation parameters are included in the caption of Figure 3.

Little information could be obtained about the analogous isomerization of the neutral forms. In principle, a voltammogram of TBP^+ reduction obtained at slow scan rates should show growth of a similar shoulder on the second half cycle, the positive-going scan. This would be due to the reaction pathway

(8) (a) Murray, R. C.; Blum, L.; Liu, A. H.; Schrock, R. R. *Organometallics* **1985**, *4*, 953–954. (b) Murray, R. C.; Schrock, R. R. *J. Am. Chem. Soc.* **1985**, *107*, 4557–4558. (c) O'Regan, M. B.; Liu, A. H.; Finch, W. C.; Schrock, R. R.; Davis, W. M. *J. Am. Chem. Soc.* **1990**, *112*, 4331–4338. (d) Glassman, T. E.; Vale, M. G.; Schrock, R. R. *Inorg. Chem.* **1992**, *31*, 1985–1986. (e) Glassman, T. E.; Vale, M. G.; Schrock, R. R. *J. Am. Chem. Soc.* **1992**, *114*, 8098–8109. (f) Schrock, R. R.; Glassman, T. E.; Vale, M. G.; Kol, M. *J. Am. Chem. Soc.* **1993**, *115*, 1760–1772.

(9) Lerke, S. A.; Evans, D. H.; Feldberg, S. W. *J. Electroanal. Chem.* **1990**, *296*, 299–315.

Table 1. Summary of Rate and Equilibrium Constants[a]

temp, K	$K^+/(k_f^+)^{1/2}$, $s^{1/2}$	k_f^+, s^{-1}	K^+
308	2.7	(9.8×10^5)	2.7×10^3
303	3.6	(8.0×10^5)	3.2×10^3
298	4.7	(6.3×10^5)	3.7×10^3
293	6.2	(5.0×10^5)	4.4×10^3
243	(2.0×10^2)	3.1×10^4	3.4×10^4
238	(3.3×10^2)	2.4×10^4	5.1×10^4
233	(5.2×10^2)	1.5×10^4	6.3×10^4
228	(8.3×10^2)	1.0×10^4	8.4×10^4

[a] Values in parentheses were obtained by extrapolation of linear plots of log (parameter) *vs* $1/T$.

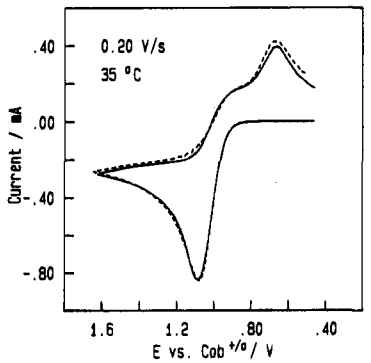

Figure 3. Cyclic voltammogram of *ca.* 5 mM $W(\eta^5\text{-}C_5(CH_3)_5)(CH_3)_4$ in methylene chloride containing 0.40 M Bu_4NPF_6: (—) background-corrected voltammogram; (- - -) simulation with $E^\circ_1 = 1.20$ V, $E^\circ_2 = 0.66$ V, $\alpha_1 = \alpha_2 = 0.5$, $k_{s1}/D^{1/2} = 240$ $s^{-1/2}$, $k_{s2}/D^{1/2} = 18$ $s^{-1/2}$, $K^+/(k_f^+)^{1/2} = 2.7$ $s^{1/2}$, $1/K^\circ(k_b^\circ)^{1/2} = 490$ $s^{1/2}$. Conditions: 0.70-cm-diameter platinum-disk electrode, 0.20 V/s, 308 K. As the exact concentration and diffusion coefficient were not known, the simulation was scaled to match the anodic peak with the experimental value.

SP → TBP → TBP^+. In agreement with the results of Liu,[10] no evidence of such a shoulder could be seen in a voltammogram at 0.05 V/s (not shown) putting a lower limit of 10 on $1/K^\circ(k_b^\circ)^{1/2}$ at room temperature, a limit evaluated through the use of simulations as above. It should be noted that the voltammetry of TBP^+ was fully consistent with the results obtained from the cyclic voltammetric study of SP as in Figure 3. Reduction of TBP^+ shows a pre-peak on the first negative-going half cycle that is due to the reaction pathway $TBP^+ \rightarrow SP^+ \rightarrow$ SP. This pre-peak was most prominent at the slowest scan rates, and digital simulations using the previously determined parameters (Table 1) provided good fits of the data.

In an effort to place limits on reaction rates among the neutral forms, two-cycle voltammograms of SP oxidation were performed at fast scan rates. On the positive-going half cycle of the second cycle, it should be possible to detect the oxidation of TBP to TBP^+ if the experiment is fast enough to overcome the TBP → SP reaction. Failure to detect a peak for TBP at 10^4 V/s (298 K) puts a lower limit of 4×10^4 s^{-1} on k_b° as judged by digital simulation. Combined with the above limit on $1/K^\circ(k_b^\circ)^{1/2}$, the result indicates that $K^\circ \leq 5 \times 10^{-4}$, consistent with the observation that SP is the only detectable isomer.[7]

The results obtained at slow scan rate for oxidation of SP (Figure 3) have provided compelling evidence that the reaction must be a two-step electron-transfer reaction. It would be even more convincing if it were possible to detect the putative SP^+ *prior* to its isomerization to TBP^+ rather than indirectly through the reduction current seen for SP^+ by way of the isomerization back reaction.

(10) Liu, A. H., Ph.D. Thesis, Massachusetts Institute of Technology, 1988.

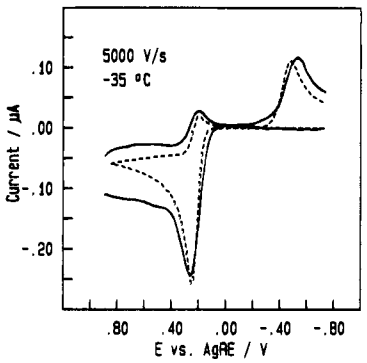

Figure 4. Cyclic voltammogram of *ca.* 8 mM $W(\eta^5\text{-}C_5(CH_3)_5)(CH_3)_4$ in methylene chloride containing 0.40 M Bu_4NPF_6: (—) background-corrected voltammogram; (- - -) simulation with $k_f^+ = 2.4 \times 10^4$ s^{-1}; electrode reaction 1 considered to be reversible, reaction 2 irreversible ($\alpha_2 = 0.5$) and the potentials adjusted to place the peaks in the observed positions. Conditions: 10-μm-diameter platinum-disk electrode, 5000 V/s, 238 K.

The direct detection of SP^+ was achieved by fast-scan cyclic voltammetry using microelectrodes at low temperature. An example is shown in Figure 4, where the background-corrected voltammogram for oxidation of SP is shown for 5×10^3 V/s and 238 K. Clearly on the reverse scan a small reduction peak is seen near the potential of the anodic peak. This peak is assigned to the reduction of SP^+ that has not been able to isomerize to TBP^+. The peak for reduction of TBP^+ appears at −0.5 V and is larger than the peak due to SP^+ at this scan rate signifying that most of the SP^+ has isomerized. When the scan rate was increased to 10^4 V/s, the two reduction peaks were almost equal in height as less SP^+ was able to isomerize during the faster experiment.

Comparison of simulation with the experimental data is also shown in Figure 4 where the value of k_f^+ was taken to be 2.4×10^4 s^{-1}. The quality of fit is poorer than seen with the slow scan rate simulations which is mainly due to inadequate background correction. The background signal (principally current for charging the electrical double layer) was recorded in separate experiments using only solvent and supporting electrolyte ("blank" signal) and later subtracted from the voltammogram obtained with SP present to give the background-corrected data. At the rapid scan rates used in these studies, the background is much larger than the faradaic current from oxidation of SP. For example, the background current was 3.3 times as large as the anodic peak current at 10^4 V/s. Even slight errors in reproducing the background signals in the "blank" voltammograms can cause substantial distortions in the corrected data.

For this reason we concentrated on simulating the relative heights of the SP^+ and TBP^+ peaks in the low-temperature voltammograms and did not focus on the other regions of the voltammogram. The relative peak heights were accurately reproduced in the range of 2×10^3 to 2×10^4 V/s and the results for k_f^+ are included in Table 1 for four temperatures from 228 to 243 K.

Arrhenius plots of the four low-temperature values of k_f^+ were linear ($r = 0.990$; $\Delta H^{\circ *} = 7.9$ kcal/mol; $\Delta S^{\circ *} = -5$ cal mol^{-1} K^{-1})[11] and allowed estimation of k_f^+ by extrapolation to each

(11) Based on the thermodynamic expression of activated-complex theory: $k = (k_B T/h) \exp(-\Delta G^{\circ *}/RT)$ and $\Delta G^{\circ *} = \Delta H^{\circ *} - T\Delta S^{\circ *}$ where k_B is Boltzmann's constant, h is Planck's constant, and $\Delta G^{\circ *}$, $\Delta H^{\circ *}$, and $\Delta S^{\circ *}$ are the activation free energy, enthalpy, and entropy, respectively.

(12) (a) Based[12b] on a pre-exponential factor, A, of 10^4 cm/s in $k_s = A \exp(-\Delta G^{\circ *}/RT)$. (b) For a discussion of the pre-exponential factor in electrode kinetics see: Weaver, M. J. In *Comprehensive Chemical Kinetics*; Compton, R. G., Ed.; Elsevier: Amsterdam, 1987; Vol. 27, pp 1−60.

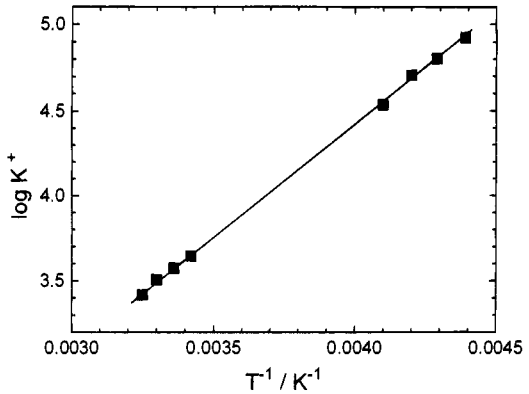

Figure 5. Dependence of K^+ on temperature.

of the four higher temperatures (cf. Table 1). Similarly, plots of log $[K^+/(k_f^+)^{1/2}]$ *vs* $1/T$ were also linear ($r = 0.999$) and afforded estimates of the grouped parameter at the four low temperatures. Combination of the values of k_f^+ and $K^+/(k_f^+)^{1/2}$ allowed calculation of K^+ at each temperature (Table 1). The data for both low- and high-temperature data sets fit the same straight line (Figure 5) whose slope gives $\Delta H^\circ = -6.03 \pm 0.04$ kcal mol for conversion of SP^+ to TBP^+ ($\Delta S^\circ = -3.97 \pm 0.05$ cal mol^{-1} K^{-1}).

Discussion

Discussion of the factors that differentiate one-step from two-step reactions requires knowledge of the relative energies of possible intermediates.[14] Only results at 298 K will be discussed. Fits of simulation to the slow scan rate data provide an estimate of $E^\circ_1 = +1.20$ V *vs* the cobaltocenium/cobaltocene couple (Cob). From Table 1, $K^+ = 3.7 \times 10^3$ for equilibrium between the two isomeric cations. These two quantities may be combined to obtain the reversible formal potential for the reaction connecting the preferred isomers of each oxidation state, SP and TBP^+. This potential, E°_{ov} (Scheme 1), is given[9] by $E^\circ_{ov} = E^\circ_1 + (RT/F) \ln [(1 + K^\circ)/(1 + K^+)] = +0.99$ V *vs* Cob (assuming $K^\circ \ll 1$ as shown earlier). Thus, the reversible potential for the direct oxidation of SP to TBP^+ precedes the potential for oxidation of SP to SP^+ by 0.21 V.

It was only possible to place an upper limit on K°, *i.e.*, $K^\circ \leq 5 \times 10^{-4}$. For purposes of illustration, $K^\circ = 5 \times 10^{-4}$ gives $E^\circ_2 = +0.79$ V from $E^\circ_{ov} = E^\circ_2 + (RT/F) \ln [(1 + 1/K^\circ)/(1 + 1/K^+)]$.[9] This is the upper limit for E°_2, the reversible formal potential for the TBP/TBP^+ couple. So, TBP is at least 0.41 V more easily oxidized than SP.

The factor that is of interest here is the observation that oxidation of SP occurs by the two-step process in which SP is oxidized to SP^+ followed by isomerization to TBP^+ in spite of the fact that direct one-step oxidation of SP to TBP^+ requires 5 kcal/mol less energy (0.21 V). The explanation must be found in the relative barrier heights for the two processes.

Turning to the kinetics of the redox process, simulations of both the slow and fast scan data for the oxidation of SP indicate that the standard heterogeneous electron-transfer rate constant for the SP/SP^+ reaction is quite large, *ca.* 1 cm/s at 298 K, indicative of a reversible electron-transfer reaction. This corresponds to an activation free energy of 5.5 kcal/mol for this reaction.[12]

The second step of the observed two-step oxidation of SP to TBP^+ is the thermal isomerization of SP^+ to TBP^+ ($\Delta G^\circ_{298} =$ −4.9 kcal/mol) whose free energy of activation[11] is 9.5 kcal/mol at 298 K (from Table 1). Thus, the free energy barrier separating SP^+ from TBP^+ is 4.9 + 9.5 = 14.4 kcal/mol. This number is similar to the free energy of activation for methyl scrambling in TBP^+ (15.0 kcal/mol) as determined by ^1H NMR, a fact which has been suggested to indicate that SP^+ is an intermediate in the methyl-scrambling process.[7]

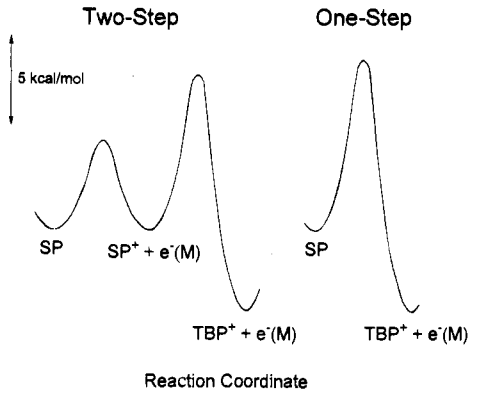

Figure 6. Schematic diagram of barriers for the two-step and one-step oxidation of $W(\eta^5\text{-}C_5(CH_3)_5)(CH_3)_4$. The diagrams correspond to the case where the electrode potential equals the formal potential of the SP^+/SP couple, E°_1, and the direct reaction is 0.21 V (5 kcal/mol) downhill. The estimated minimum barrier for the one-step reaction is more than sufficient to prevent its occurrence.

A schematic representation of the sequential barriers in the two-step reaction is given in Figure 6 which corresponds to conditions prevailing at the reversible formal potential for the SP/SP^+ couple, E°_1, *i.e.*, the free energies of SP and $SP^+ + e^-(M)$ are shown at the same level.

What can be said about the barrier for the one-step electron-transfer reaction, SP → $TBP^+ + e^-$? First, note that the experimentally observed oxidation peak is due to the two-step oxidation by which SP is oxidized to SP^+ followed by isomerization at all scan rates. One can be certain that the oxidation peaks are not due to the irreversible one-step oxidation because the peaks are much too sharp for an irreversible process, being close to the shape predicted for a reversible reaction (Figure 4) or a reversible reaction followed by fast isomerization (Figures 1 and 3). The reason that the reaction does not proceed by the direct one-step mechanism is that the inherent rate of this reaction is so small that the overpotential for the process is sufficient to shift the oxidation to those potentials where the two-step oxidation occurs instead. Thus the hypothetical oxidation peak potential for the one-step reaction must be equal or positive of the observed peak potential. The latter is dependent upon the scan rate[13] but in all cases it occurs at potentials significantly more positive than E°_{ov}, *i.e.*, there is always an overpotential for the direct reaction.

For example, at 1 V/s, the observed peak potential, $E_{p,a}$, is about 200 mV positive of E°_{ov}. The peak potential for an irreversible oxidation, $E_{p,a}$, is given by eq 1 in which $k_{s,ov}$ is the standard heterogeneous electron transfer rate constant, α_{ov} is the electron transfer coefficient, v is the scan rate, and D is the

$$E_{p,a} = E^\circ_{ov} + \frac{RT}{F}\left(0.780 + \ln\sqrt{\frac{D\alpha_{ov}Fv}{RT}} - \ln k_{s,ov}\right) \quad (1)$$

diffusion coefficient of the SP reactant.[13] Taking $E_{p,a} - E^\circ_{ov} = 0.20$ V, $\alpha_{ov} = 0.5$, $D = 10^{-5}$ cm^2/s, and $v = 1$ V/s, a maximum value of $k_{s,ov} = 1.3 \times 10^{-5}$ cm/s is obtained which corresponds[12] to a minimum activation free energy of 12 kcal/mol. A schematic representation of the barrier for the one-step reaction is also shown in Figure 6.

(13) Nicholson, R. S.; Shain, I. *Anal. Chem.* **1964**, *36*, 706−723.
(14) Brunschwig, B. S.; Sutin, N. *J. Am. Chem. Soc.* **1989**, *111*, 7454−7465.
(15) Fitch, A.; Evans, D. H. *J. Electroanal. Chem.* **1986**, *202*, 83−92.

Thus, in order to account for the preference for the two-step as opposed to direct electron transfer, it is necessary that the barrier for the latter exceeds about 12 kcal/mol. Is this a reasonable value? The principal components of the activation free energy for an electron-transfer reaction are the contributions of the outer and inner reorganization energies, the former associated with changes in solvation upon creation of the TBP^+ cation and the latter related to changes in nuclear configuration, *i.e.*, conversion of the SP structure to that of TBP^+. The contribution of the outer reorganization energy should be about the same as that assigned to the SP/SP^+ couple, 5.5 kcal/mol. The inner-shell contribution must provide at least 6−7 kcal/mol additional free energy of activation but estimation of this contribution is more problematic. The 9.5-kcal/mol barrier for the SP^+ to TBP^+ conversion (*see above*) indicates that *at least in the cations* there is a very significant resistance to the changes in structure needed to go from the SP structure of the reactant to the TBP structure of the product. For the neutral species, our results show that the free energy of TBP is at least 4.5 kcal/mol above SP (from the result that $K^\circ \leq 5 \times 10^{-4}$) so the barrier to change the SP structure to TBP may also be quite large. These results suggest that it is reasonable that the contribution of the inner reorganization energy is large enough to provide the 6−7 kcal/mol needed to explain the observation that the barrier for the direct oxidation of SP to TBP^+ is greater than 12 kcal/mol, causing its overpotential to be large enough to allow the two-step reaction to proceed instead of one-step oxidation. This redox couple appears to be an excellent candidate for high-level calculations of preferred structures of neutral and cation as well as their energies. Calculations for organic neutrals and radical ions have proven useful in correlating and rationalizing electron-transfer kinetics[3,4c,5] but the present organometallic species with their third-row transition metal core would present a more formidable challenge.

Experimental Section

Reagents. We gratefully acknowledge the donation of samples of $W(\eta^5\text{-}C_5(CH_3)_5)(CH_3)_4$ and $[W(\eta^5\text{-}C_5(CH_3)_5)(CH_3)_4]BF_4$ by Marie O'Regan and Professor R. R. Schrock (Massachusetts Institute of Technology). These materials were stored at −35 °C in a drybox. Dichloromethane (Fisher) was dried over molecular sieves (Mallinckrodt, 4A), distilled from calcium hydride or P_2O_5, and degassed before being taken into the drybox. Tetra-*n*-butylammonium hexafluorophosphate (Bu_4NPF_6) was obtained from Aldrich, recrystallized three times from ethanol, vacuum dried at 85 °C for at least 18 h, and stored in a desiccator. Cobaltocenium hexafluorophosphate (Aldrich) was used as received.

Electrochemical Instrumentation. Electrochemical instrumentation for scan rates up to about 100 V/s consisted of an EG&G Princeton Applied Research (PAR) Model 175 programmer. Positive feedback compensation of solution resistance was employed. At scan rates up to 0.5 V/s, the voltammograms were recorded with a BD 90 902/902 Kipp & Zonen XY recorder. All data at faster scan rates were acquired using a Model 4094 or 4094C Nicolet digital oscilloscope.

For experiments at scan rates greater than about 100 V/s, a PAR 173 potentiostat was used with a fast home-built current-to-voltage converter[15] and a Hewlett Packard Model 3314A function generator[16,17] to provide the triangular waveform. The cell was operated in a two-electrode configuration[15,17] with the potential of the counter electrode poised by connection to the silver reference electrode. Signal averaging of 100−300 individual voltammograms was used with the rest time between voltammograms being at least ten times the sweep duration.

For scan rates less than 0.5 V/s, a large (0.70- or 0.50-cm diameter) platinum-disk working electrode was used. For faster scan rates, microelectrodes (10 to 200 μm diameter) were used.[18] Between experiments these electrodes were polished with 0.05−μm alumina (Buehler) and placed in concentrated nitric acid for 5 min. A coil of platinum wire served as counter electrode. The silver reference electrode (AgRE) comprised a silver wire in contact with about 0.01 M $AgClO_4$ and 0.40 M Bu_4NPF_6 in dichloromethane. Potential measurements at temperatures near ambient were also referenced to the reversible potential of the cobaltocenium/cobaltocene couple as an internal standard.

All electrochemical measurements were performed in a Vacuum Atmospheres drybox. Temperature was monitored with a Trendicator digital thermometer with the thermocouple junction placed within the cell. The thermometer was calibrated at −78, 0, and 100 °C. Temperature control was achieved by passing nitrogen gas through a glass jacket that surrounded the cell sample compartment. The temperature of the nitrogen gas was controlled by passing it through a coil of copper tubing immersed in liquid nitrogen (or a temperature-controlled water bath). The cell temperature was then adjusted by controlling the nitrogen flow rate.

Digital Simulations. Simulation of cyclic voltammograms corresponding to the square scheme encountered in this work were achieved using either standard explicit finite difference simulations or the fast quasi-explicit finite difference method.[9]

Acknowledgment. This research was supported by the National Science Foundation, Grant No. CHE9322773.

JA952876P

(16) Smith, D. K.; Strohben, W. E.; Evans, D. H. *J. Electroanal. Chem.* **1990**, *288*, 111−128.

(17) Bowyer, W. J.; Engelman, E. E.; Evans, D. H. *J. Electroanal. Chem.* **1989**, *262*, 67−82.

(18) Bowyer, W. J.; Evans, D. H. *J. Electroanal. Chem.* **1988**, *240*, 227−237.